Fuzzy sliding-mode control of a human arm in the sagittal plane with optimal trajectory

Fateme Fotouhi Ardakani | **Ramin Vatankhah** ⓘ | **Mojtaba Sharifi**

School of Mechanical Engineering, Shiraz University, Shiraz, Iran.

Correspondence
Ramin Vatankhah, School of Mechanical Engineering, Shiraz University, Shiraz, Iran.
Email: rvatankhah@shirazu.ac.ir

Patients with spinal cord injuries cannot move their limbs using their intact muscles. A suitable controller can be used to move their arms by employing the functional electrical stimulation method. In this article, a fuzzy exponential sliding-mode controller is designed to move a musculoskeletal human arm model to track an optimal trajectory in the sagittal plane. This optimal arm trajectory is obtained by developing a policy for the central nervous system. In order to specify the optimal trajectory between two points, two dynamic and static optimal criteria are applied simultaneously. The first dynamic objective function is defined to minimize the joint torques, and the second static optimization is offered to minimize the muscle forces at each moment. In addition, fuzzy logic is used to tune the sliding-surface parameter to enable an appropriate tracking performance. Simulation results are evaluated and compared with experimental data for upward and downward movements of the human arm.

KEYWORDS
fuzzy SMC controller, human musculoskeletal arm model, optimal arm movement, sagittal plane, trajectory tracking

1 | INTRODUCTION

Intact human arms can perform common movements that enable them to pick up and put down objects, lift an object to put on a shelf, wave, and so on. These tasks are applied in the sagittal plane immediately without considering the trajectories between the initial and final points of their movements. In fact, the central nervous system (CNS) predicts these trajectories using the large amount of information that is obtained from the environment and the body feedback signals. For example, this information can be the initial and final points of the arm movements, the arm velocity, and the muscles' configurations and forces. In recent decades, many studies have aimed to investigate the function of the CNS and predict the human arm trajectories and to understand the manner in which the muscles are activated. Nevertheless, the study of the CNS strategy while analyzing the feedback

sensory data and producing motor commands to gain the desired behavior remains an issue to be clarified [1].

The damaged nerves of poststroke patients can be activated by electrical currents. This method is called functional electrical stimulation (FES) [2]. In this approach, the magnitude of this current is important as it affects the limb movements. Therefore, a proper controller can tune the intensity of this electrical stimulation to enable it to perform the desired task. In order to help these patients to move their arms toward the goal with minimum fatigue, the optimal trajectory of the human limb can be investigated.

The optimization approach in the field of biomechanics is a suitable method of predicting the CNS policy [3–5]. For this purpose, different biological objective functions can be expressed. The minimum-jerk criterion was used to optimize the hand with 1 and 2 degrees of freedom (DOF) in [6,7]. Minimizing the rate of the joint torque was proposed in order

to predict the 2 DOF human arm motions [8,9]. The minimum-acceleration criterion was also used to predict the arm-reaching movements [10]. In [11], the arm trajectory in the sagittal plane was evaluated by minimizing metabolic energy costs for the human arm model using uniarticular and biarticular muscles. Moreover, an approximate optimal feedback control (OFC) was considered to simulate the pattern of limb stiffness for the musculoskeletal arm model [12]. In [13], the muscle activation effort and metabolic energy were considered as 2 time-integral objective functions to predict a periodic forearm motion. In addition, the linear-quadratic-Gaussian (LQG) method was considered as an optimal control for the two-DOF arm model [14]. A physiological objective function for minimizing the metabolic energy expenditure was expressed in order to analyze human arm movement in crank-rotation tasks [15]. In [16], the optimal arm trajectory was found for arm-reaching movements using an optimal torque control method based on arm dynamics. In addition, the quadratic function of muscle stresses plus the total movement duration was proposed as an objective function to investigate the optimal performance and to predict the optimal trajectory of a planar human-like musculoskeletal arm model by considering the joint and muscle constraints [17,18]. In our proposed objective functions, torques and muscle forces are minimized. These objective functions are defined according to a comparison of related works in the horizontal plane. The results of these works with body experiments indicate that these objective functions can predict the CNS policy appropriately.

Many control strategies have been proposed to understand the dynamics of human arm models. An iterative learning control method was studied in [19] to acquire the adequate internal force for nonlinear muscle dynamics in a 2-DOF arm model. An adaptive optimal neuro-fuzzy controller was expressed in [20] for a multi-input multi-output (MIMO) musculoskeletal human arm model with six muscles. In [21], an FES controller was developed to restitute the ability for paralyzed people to perform functional interaction tasks. In addition, for a planar arm actuated by pneumatic muscle (PM) actuators, multiple-input sliding-mode techniques were applied [22]. In [23], the modified sliding mode with exponential reaching law (mSMERL) was presented to control the nonlinear dynamics of a 7-DOF exoskeleton arm. In [24], the exponential sliding-mode controller was investigated for a musculoskeletal human arm model in the presence of gravitational effects. Chattering is a major issue involving the use of a sliding-mode control (SMC) strategy for dynamical systems because it damages the mechanical components.

To minimize the chattering issue, different methods were proposed, such as replacing the sign function with saturation [25] or a continuous hyperbolic tangent function [26], applying Quasi-SMC [27] and fuzzy mathematics [28].

Accordingly, the combination of an SMC algorithm and fuzzy logic developed for robot manipulators was investigated in [28]. In addition, a fuzzy approximation-based adaptive SMC was considered for uncertain nonlinear underactuated systems [29]. Therefore, the SMC approach has been utilized for many dynamic systems owing to its simplicity, instant response, appropriate transient performance, and insensitivity to parametric changes and uncertainties within the system. Furthermore, in the authors' previous work, the appropriate performance and instant response of this controller were represented and investigated. Based on its advantages, the fuzzy exponential sliding-mode control (FESMC) was employed in this work. A fuzzy logic was also used to tune the sliding-surface parameter such that it has a rapid response.

In this research, two dynamic and static optimal criteria are proposed in parallel to minimize the muscle fatigue in the sagittal plane for a musculoskeletal human arm model. In this plane, the gravitational force affects the dynamic equation and the optimal response. The first dynamic objective function is defined to minimize the joint torques, and the second static optimization is defined to minimize the muscle forces from the obtained optimal torques at each moment. These parallel optimizations are proposed to make the results closer to real human arm trajectories.

The paper is organized as follows. The kinematics and dynamics of the 2-DOF musculoskeletal human arm model are presented in Section 2. The control scheme, which includes the fuzzy exponential sliding-mode controller and two optimal criteria are designed in Section 3. Section 4 presents the simulation results and their evaluations. Finally, the conclusion is given in Section 5.

2 | DYNAMICS OF MUSCULOSKELETAL HUMAN ARM MODEL

The 2-DOF musculoskeletal human arm model that is proposed in this study has an upper arm and forearm segments, two joints, and six muscles. The kinematics of the model is shown in Figure 1. The model simulates the planar motion of the human upper-limb in the sagittal (vertical) plane. In this plane, the shoulder and elbow have their flexion-extension movements. The model contains six muscles, namely the anterior and posterior deltoid (l_1, l_2), brachialis (l_3), lateral and long head of the triceps (l_4, l_5), and long head of the biceps (l_6). These muscles can only cause tensile forces that actuate the shoulder and elbow joints. The overall movements of the system are assumed in the sagittal plane so that the gravity affects the arm's movements. The shoulder angle is within the range of −60° to 180°, and the elbow angle is within the range of 0° to 170°. As shown in Figure 1, the long head of the triceps and long head of the biceps are biarticular, and the
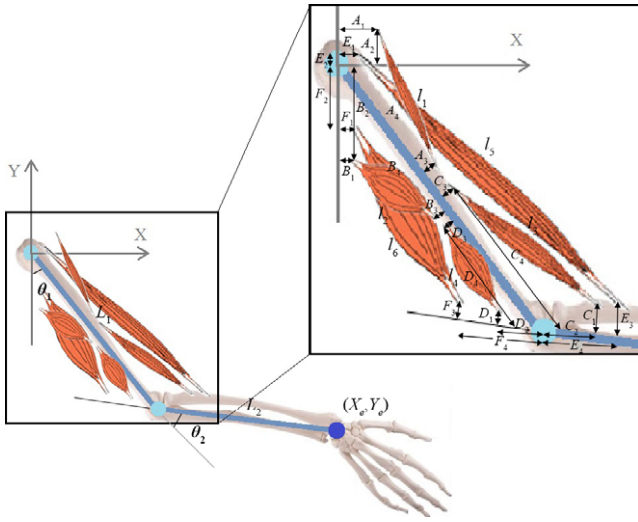
FIGURE 1 Two-degree of freedom musculoskeletal arm model in the sagittal plane with two links and six muscles

other muscles are monoarticular. In addition, the muscles' moment arms vary according to the joint angles.

The physical parameters and variables were obtained from related works. The physiological cross-sectional area (PCSA) for each muscle was obtained from [30,31]. The muscle's configuration and the position of their attachments were obtained from [32,33], while the length, mass, and inertia of the upper arm and forearm segments are considered the same as those in [11].

2.1 | Kinematics of muscle-joint space

The distances between the insertion points of the muscles are expressed as the lengths of the muscles. The relations between these lengths l_i and the joint angles θ_i are formulated as follows:

$$
\mathbf{l} = [l_1, l_2, l_3, l_4, l_5, l_6]^T
$$

$$
= \begin{bmatrix}
[(A_2 + A_4\cos(\theta_1) - A_3\sin(\theta_1))^2 + (A_1 - A_4\sin(\theta_1) - A_3\cos(\theta_1))^2]^{\frac{1}{2}} \\
[(B_1 - B_4\cos(\theta_1) - B_3\sin(\theta_1))^2 + (B_1 - B_4\sin(\theta_1) + B_3\cos(\theta_1))^2]^{\frac{1}{2}} \\
[(C_2 + C_4\cos(\theta_2) - C_3\sin(\theta_2))^2 + (C_1 - C_4\sin(\theta_2) - C_3\cos(\theta_2))^2]^{\frac{1}{2}} \\
[(D_2 + D_4\cos(\theta_2) - D_3\sin(\theta_2))^2 + (D_1 - D_4\sin(\theta_2) - D_3\cos(\theta_2))^2]^{\frac{1}{2}} \\
\begin{bmatrix} (E_2 + E_4\cos(\theta_1 + \theta_2) - E_3\sin(\theta_1 + \theta_2) + L_1\cos(\theta_1))^2 \\ +(E_1 - E_4\sin(\theta_1 + \theta_2) - E_3\cos(\theta_1 + \theta_2) - L_1\sin(\theta_1))^2 \end{bmatrix}^{\frac{1}{2}} \\
\begin{bmatrix} (F_2 + F_4\cos(\theta_1 + \theta_2) - F_3\sin(\theta_1 + \theta_2) + L_1\cos(\theta_1))^2 \\ +(F_1 - F_4\sin(\theta_1 + \theta_2) - F_3\cos(\theta_1 + \theta_2) - L_1\sin(\theta_1))^2 \end{bmatrix}^{\frac{1}{2}}
\end{bmatrix}
\tag{1}
$$

where the parameters A_i, B_i, C_i, D_i, E_i, and F_i ($i = 1, 2, 3,$ and 4) are represented in Figure 1. The magnitudes of these parameters are presented in Table 1.

Taking the first derivative of (1) with respect to time yields:

$$
\dot{\mathbf{l}} = -\mathbf{J}(\boldsymbol{\theta})^T\dot{\boldsymbol{\theta}},
\tag{2}
$$

where $\mathbf{J}(\boldsymbol{\theta})^T \in \Re^{6\times2}$ is a Jacobian matrix that relates the joint angular velocity ($\dot{\boldsymbol{\theta}} \in \Re^2$) to the muscle contractile velocity ($\dot{\mathbf{l}} \in \Re^6$).

From the principle of virtual work, the relation between the joint torques $\boldsymbol{\tau} = [\tau_1 \ \tau_2]^T \in \Re^2$ and tensile forces of the muscles $\mathbf{f} = [f_1 \ f_2 \ f_3 \ f_4 \ f_5 \ f_6]^T \in \Re^6$ can be obtained as:

$$
\boldsymbol{\tau} = \mathbf{J}(\boldsymbol{\theta})\mathbf{f}.
\tag{3}
$$

2.2 | Dynamics of musculoskeletal arm model in sagittal plane

The dynamics of 2-DOF musculoskeletal arm models can be described in joint space by Lagrange's equation of motion as follows:

$$
\mathbf{M}(\boldsymbol{\theta})\ddot{\boldsymbol{\theta}} + \mathbf{C}(\boldsymbol{\theta}, \dot{\boldsymbol{\theta}}) + \mathbf{G}(\boldsymbol{\theta}) = \boldsymbol{\tau}
\tag{4}
$$

where $\ddot{\boldsymbol{\theta}} \in \Re^2$, $\dot{\boldsymbol{\theta}} \in \Re^2$, $\boldsymbol{\theta} \in \Re^2$ are the angular accelerations, velocities, and positions of the joints, respectively. $\mathbf{M}(\boldsymbol{\theta}) \in \Re^{2\times2}$ is the inertia matrix, which is symmetric and positive definite, $\mathbf{C}(\boldsymbol{\theta}, \dot{\boldsymbol{\theta}}) \in \Re^{2\times1}$ is a Coriolis and centrifugal and friction torques matrix, and $\mathbf{G}(\boldsymbol{\theta}) \in \Re^{2\times1}$ is a gravity vector. For the 2-link model in the sagittal plane, as shown in Figure 1, these matrices can be obtained as:

$$
\mathbf{M}(\boldsymbol{\theta}) = \begin{bmatrix} M_{11} & M_{12} \\ M_{21} & M_{22} \end{bmatrix},
\tag{5}
$$

$$
M_{11} = m_1 L_{g_1} + I_1 + m_2(L_{g_2}^2 + L_1^2) + I_2 + 2m_2 L_1 L_{g_2}\cos(\theta_2),
$$
$$
M_{12} = M_{21} = m_2 L_{g_2}^2 + I_2 + m_2 L_1 L_{g_2}\cos(\theta_2),
$$
$$
M_{22} = m_2 L_{g_2}^2 + I_2,
$$

$$
\mathbf{C}(\boldsymbol{\theta}, \dot{\boldsymbol{\theta}}) = \begin{bmatrix} -m_2 L_1 L_{g2}(2\dot{\theta}_1\dot{\theta}_2 + \dot{\theta}_2^2)\sin(\theta_2) + c_1\dot{\theta}_1 \\ m_2 L_1 L_{g2}\dot{\theta}_1^2\sin(\theta_2) + c_2\dot{\theta}_2 \end{bmatrix},
\tag{6}
$$

$$
\mathbf{G}\boldsymbol{\theta} = \begin{bmatrix} (m_1 L_{g_1} + m_2 L_1)g\sin(\theta_1) + m_2 g L_{g_2}\sin(\theta_1 + \theta_2) \\ m_2 g L_{g_2}\sin(\theta_1 + \theta_2) \end{bmatrix},
\tag{7}
$$

TABLE 1 Parameters of Figure 1 (muscle locations)

Muscle 1	Muscle 2	Muscle 3	Muscle 4	Muscle 5	Muscle 6
$A_1 = 1.18$	$B_1 = 1.34$	$C_1 = 1.44$	$D_1 = 1.42$	$E_1 = 2.78$	$F_1 = 3.65$
$A_2 = 3.12$	$B_2 = 2.21$	$C_2 = 4.63$	$D_2 = 1.10$	$E_2 = 1.53$	$F_2 = 1.15$
$A_3 = 2.13$	$B_3 = 2.92$	$C_3 = 0.57$	$D_3 = 0.42$	$E_3 = 0.11$	$F_3 = 0.17$
$A_4 = 12.37$	$B_4 = 10.85$	$C_4 = 18.13$	$D_4 = 25.27$	$E_4 = 5.19$	$F_4 = 1.72$

where c_1 and c_2 are the viscous friction coefficients in the shoulder and elbow joints, respectively. m_i, I_i, L_i, and L_{gi} ($i = 1, 2$) are the mass, moment of inertia, length, and mass center position of the upper arm and forearm segments, respectively. g is the gravitational acceleration.

According to the kinematics of muscle-joint space (Section 2.1), the joints torques are expressed in (3). Thus, Equation (4) can be rewritten as:

$$\mathbf{M}(\boldsymbol{\theta})\ddot{\boldsymbol{\theta}} + \mathbf{C}(\boldsymbol{\theta},\dot{\boldsymbol{\theta}}) + \mathbf{G}(\boldsymbol{\theta}) = \mathbf{J}(\boldsymbol{\theta})\mathbf{f}. \tag{8}$$

3 | CONTROL SCHEME

3.1 | Fuzzy exponential sliding-mode control

In this section, the fuzzy exponential sliding-mode controller is designed to track the arm trajectory of the musculoskeletal human arm model in the sagittal plane. In Section 3.2, the optimal arm trajectory in this plane was obtained. Therefore, individuals with spinal cord injuries can move their arms between two points on the optimal trajectory that "normal" individuals move their arms on.

For this purpose, first, the exponential sliding-mode controller is expressed, and then the fuzzy logic was used to tune the sliding-surface parameter.

3.1.1. | Exponential sliding-mode controller

The dynamic behavior of musculoskeletal human arm model in the sagittal plane was expressed in (4). Now, $\ddot{\theta}$ should be extracted as follows in order to perform this controller scheme.

$$\ddot{\boldsymbol{\theta}} = \mathbf{M}^{-1}(\boldsymbol{\theta})\big(\boldsymbol{\tau} - \mathbf{C}(\boldsymbol{\theta},\dot{\boldsymbol{\theta}}) - \mathbf{G}(\boldsymbol{\theta})\big). \tag{9}$$

Because $M(\theta)$ is a symmetric and positive definite matrix, $M^{-1}(\theta)$ always exists. The first step in the design of the sliding-mode controller is to define the sliding surface. These sliding (switching) surfaces are a function of the tracking error, where the tracking error is expressed as follow:

$$e = \theta - \theta_d. \tag{10}$$

θ_d is the desired path, which in this article, is the optimal trajectory of the human arm model that will be obtained in the next section. The sliding surface is defined as:

$$S = \lambda e + \dot{e}. \tag{11}$$

Owing to the first-order differential Equation (11), when the system states slide along the line $S = 0$, e and $\dot{e}$ converge to zero. In addition, λ represents the convergence rate.

In order to satisfy the Lyapunov stability, the Lyapunov candidate for this model is considered as:

$$E = \frac{1}{2}\mathbf{R}^T\mathbf{R} \tag{12}$$

where $\mathbf{R}$ is a vector of two sliding surfaces ($\mathbf{R} = [\lambda_1 e_1 + \dot{e}_1 \quad \lambda_2 e_2 + \dot{e}_2]^2$). E is a non-negative and continuous function that satisfies the first condition of the Lyapunov stability. In order to investigate the second condition of the Lyapunov stability, the first derivation of E should be calculated

$$\dot{E} = \mathbf{R}^T\dot{\mathbf{R}}. \tag{13}$$

To satisfy the system stability, $\dot{E}$ should be negative definite. Therefore, $\dot{\mathbf{R}}$ is usually defined as given below, where $\mathbf{K} = \text{diag}(K_1, K_2)$ is positive.

$$\dot{R} = -\mathbf{K}\text{sgn}(\mathbf{R}) \quad (i = 1, 2). \tag{14}$$

Because the sign function is a discontinuous function, we may experience the undesirable phenomenon of oscillations near the sliding surface having a finite frequency and amplitude, which is known as "chattering." To reduce the damage caused by this phenomenon, a continuous function such as the saturation can be used [25]. A boundary layer ($\boldsymbol{\delta} = [\delta_1 \; \delta_2]^T$) is defined on the neighborhood of each sliding surface, so that the convergence of the system remains between this boundary layer [34]. Therefore, $\dot{\mathbf{R}}$ is considered as:

$$\dot{\mathbf{R}} = \mathbf{K}\text{sat}\left(\frac{\mathbf{R}}{\boldsymbol{\delta}}\right). \tag{15}$$

However, when $\dot{\mathbf{R}}$ is defined as (15), the tracking performance of the system is negatively affected. Therefore, the K_i coefficient is expressed as an exponential term that adapts to the variations of the sliding function. Therefore, the system is able to tune between reducing the chattering phenomenon and improving the tracking performance [23]. Finally, $\dot{R}$ is rewritten as:

$$\dot{\mathbf{R}} = \mathbf{K}(S)\text{sat}(\frac{\mathbf{R}}{\boldsymbol{\delta}}) \tag{16}$$

where $\mathbf{K}(S) = \text{diag}(K_1(S_1), K_2(S_2))$.

$K_i(S_i)$ is defined as:

$$K_i(S_i) = \frac{k_i}{\delta_{0i} + (1 - \delta_{0i})e^{-\alpha_i|S_i|^{P_i}}} \tag{17}$$

where k_i is a discontinuous controller gain.

In addition, $0 < \delta_{0i} < 1$, $\alpha_i > 0$ and $P_i > 0$.

Now, to check the stability analysis, the derivative of the Lyapunov function is rewritten as:

$$\dot{E} = -\mathbf{R}^T\text{sat}\left(\frac{\mathbf{R}}{\boldsymbol{\delta}}\right)\mathbf{K}(\mathbf{R}) \tag{18}$$

$\dot{E}$ is always negative because the term $\mathbf{R}^T\text{sat}(\mathbf{R}/\boldsymbol{\delta})$ is obviously positive. Therefore, the stability of the system with the proposed exponential reaching law is fulfilled.

3.1.2 | Fuzzy controller for tuning λ

In order to amend the performance, such as the smaller settling time and lower overshoot, the strictly positive constant λ should be tuned in each time step. For the online tuning of this positive constant with the fuzzy controller, the Mamdani implication and center-average defuzzifier were used. In addition, e and $\dot{e}$ are considered as the input linguistic variables of fuzzy rules. For the input linguistic variable, the characters NN, N, Z, P, and PP are considered as negative large, negative, zero, positive, and positive large, respectively. Furthermore, for the output linguistic variable, the characters P, PP, and PPP are considered as positive small, positive medium, and positive large, respectively. The fuzzy rules table is shown in Table 2.

For the inputs and output, the triangular membership functions are considered, as shown in Figure 2. In addition, the range of linguistic variables for $e_1, e_2, \dot{e}_1, \dot{e}_2$ and λ are $[-0.4\ 0]$, $[-0.2\ 0]$, $[0\ 3]$, $[0\ 2]$, $[0\ 40]$, respectively.

The overall control scheme is displayed in Figure 3.

3.2 | Two criteria to obtain optimal arm trajectory

In this section, the optimal trajectory of the musculoskeletal human arm model in the sagittal plane is obtained. By tracking this optimal trajectory with the proposed fuzzy sliding-mode controller, the patients' arms can be moved in the sagittal plane as in the arms of normal persons.

The equation of motion for this 2-DOF arm model should be expressed in state-space form in order to apply the optimal control strategy. Therefore, the system dynamic is obtained as:

$$\begin{bmatrix} \dot{x}_1 \\ \dot{x}_2 \\ \dot{x}_3 \\ \dot{x}_4 \\ \dot{x}_5 \end{bmatrix} = \begin{bmatrix} g_1 \\ g_2 \\ g_3 \\ g_4 \\ g_5 \end{bmatrix} = \begin{bmatrix} x_3 \\ x_4 \\ [\mathbf{M}^{-1}(x_2)(-\mathbf{C}(x_2,x_3,x_4) - \mathbf{G}(x_1,x_2) + \mathbf{J}(x_1,x_2)\mathbf{f})]_{2\times 1} \\ g_5 \end{bmatrix}$$

(19)

where $x_1 = \theta_1$, $x_2 = \theta_2$, $x_3 = \dot{\theta}_1$, $x_4 = \dot{\theta}_2$, and x_5 is the extra state that is defined to consider the constraints of the
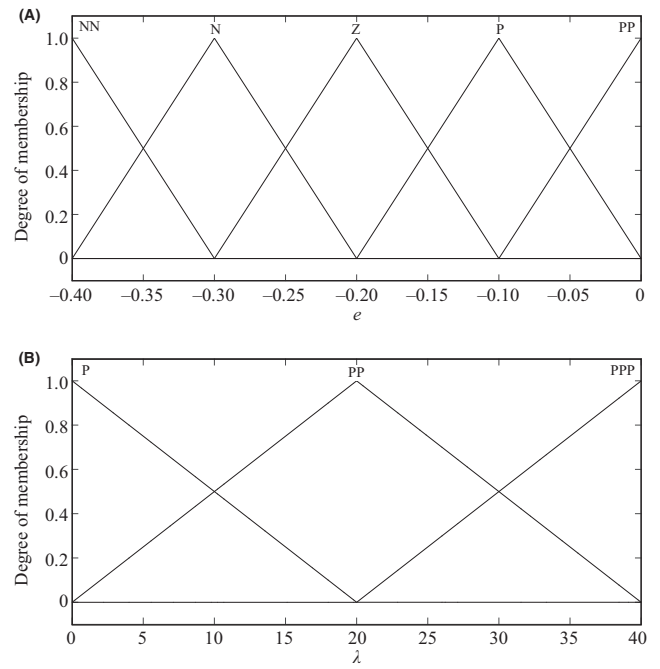

FIGURE 2 Samples of membership functions for inputs (A) and output (B)
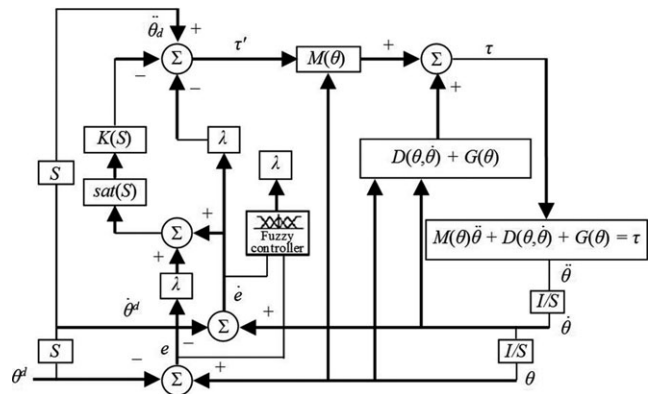

FIGURE 3 Block diagram of the control scheme

joint range of motions. Accordingly, the vector of states is expressed as $\mathbf{x} = [x_1,\ x_2,\ x_3,\ x_4,\ x_5]$ with five considered states. In addition, g_3 and g_4 are obtained from the dynamic equation as below:

$$\begin{bmatrix} g_3 \\ g_4 \end{bmatrix} = \begin{bmatrix} \ddot{\theta}_1 \\ \ddot{\theta}_2 \end{bmatrix} = [\mathbf{M}^{-1}(x_2)(-\mathbf{C}(x_2,x_3,x_4) - \mathbf{G}(x_1,x_2) + \mathbf{J}(x_1,x_2)\mathbf{f})]_{2\times 1}.$$

(20)

The dynamics of the additional state variable is expressed according to the variational approach of optimal control to satisfy the state constraints. Therefore, the state constraints should first be expressed, after which g_5 can be defined.

TABLE 2 Fuzzy rules for tuning λ

$e\backslash\dot{e}$	NN	N	Z	P	PP
NN	p	p	p	p	p
N	p	p	p	p	pp
Z	ppp	pp	p	p	p
P	pp	p	pp	pp	p
PP	pp	pp	pp	p	p

For this nonlinear musculoskeletal arm model, the state constraints are the range of the joints' motions. The ranges of the shoulder and elbow angles for their flexion-extension movement in the sagittal plane are between −60 to 180 and 0 to 170, respectively. Therefore, these constraints are considered as:

$$h(x(t),t) = \begin{bmatrix} h_1(x(t),t) \\ h_2(x(t),t) \\ h_3(x(t),t) \\ h_4(x(t),t) \end{bmatrix} = \begin{bmatrix} x_1 + 60 \\ 180 - x_1 \\ x_2 \\ 145 - x_2 \end{bmatrix} \geq 0_{4\times1}. \quad (21)$$

Now, the additional variable (state) could be defined with the following dynamics:

$$\dot{x}_{5_{(t)}} = g_5 = \sum_{i=1}^{4} [h_i(x(t),t)]^2 U(-h_i) \quad (22)$$

where $U(-h_i)$ is a unit Heaviside step function. Equation (22) states that $\dot{x}_5 \geq 0$ for all $t \in [t_0, t_f]$. From (21) and (22), when all of the constraints are within the range of the joints motion limitation, $\dot{x}_5(t) = 0$. Now, the additional variable $x_5(t)$ can be obtained by integrating $\dot{x}_5(t)$ over time as:

$$x_5(t) = \int_{t_0}^{t} \dot{x}_5(t)dt + x_5(t_0). \quad (23)$$

$\dot{x}_5(t)$ must be zero for the entire time because of the following:

1) According to Equation (22), $\dot{x}_5(t) \geq 0$ for all times.
2) The boundary conditions for this additional state variable are expressed as $x_5(t_0) = 0$ and $x_5(t_f) = 0$.

In addition, as mentioned in the previous paragraph, $\dot{x}_5(t) = 0$ when all of the state constraints are satisfied. Hence, the state constraints are satisfied automatically by defining an extra state as in (23).

To minimize the muscle fatigue, the optimal control scenario was considered. In fact, this controller simulates the CNS strategy to command the optimal movements to the human arm. For this purpose, the proposed optimal controller is considered in two steps. In the first step, the joint torques were minimized using a quadratic function of torques as the dynamic objective function. In the next step, the minimum muscles forces can be obtained using a cubic function of the muscle stresses as the static objective function.

3.2.1 | Optimal torques of shoulder and elbow joints

For the first part of the designed optimal controller, the quadratic objective function to minimize the torques vector $\boldsymbol{\tau} = [\tau_1, \tau_2]$ is expressed as:

$$J_1 = \int_{t_0}^{t_f} \frac{1}{2} \left(R_1 \tau_1^2(t) + R_2 \tau_2^2(t) \right) dt = \int_{t_0}^{t_f} \frac{1}{2} \boldsymbol{\tau}(t)^T \mathbf{R} \boldsymbol{\tau}(t) dt$$

$$= \int_{t_0}^{t_f} f(\boldsymbol{\tau}(t)) dt$$

$$(24)$$

where $\mathbf{R}$ in this objective function is a diagonal matrix as below, which allows us to value and distinguish the torques:

$$\mathbf{R} = \begin{bmatrix} R_1 & 0 \\ 0 & R_2 \end{bmatrix}. \quad (25)$$

The Hamiltonian function for this optimal controller is proposed because of the variational optimal control approach [35]. By using (19) and (24), this function can be expanded as below:

$$H = g + P^T f$$
$$= \frac{1}{2} \alpha^T R\alpha + p_1 x_3 + p_2 x_4 + p_3 f_3 + p_4 f_4 + p_5 f_5. \quad (26)$$

The vector of costates $\mathbf{p} = [p_1, \ p_2, \ p_3, \ p_4, \ p_5]^T$ is obtained from the following differential equations [35]:

$$\begin{bmatrix} \dot{p}_1 \\ \dot{p}_2 \\ \dot{p}_3 \\ \dot{p}_4 \\ \dot{p}_5 \end{bmatrix} = \begin{bmatrix} -\frac{\partial H}{\partial x_1} \\ -\frac{\partial H}{\partial x_2} \\ -\frac{\partial H}{\partial x_3} \\ -\frac{\partial H}{\partial x_4} \\ -\frac{\partial H}{\partial x_5} \end{bmatrix} = \begin{bmatrix} -p_3 \frac{\partial g_3}{\partial x_1} - p_4 \frac{\partial g_4}{\partial x_1} - p_5 \frac{\partial g_5}{\partial x_1} \\ -p_3 \frac{\partial g_3}{\partial x_2} - p_4 \frac{\partial g_4}{\partial x_2} - p_5 \frac{\partial g_5}{\partial x_2} \\ -p_1 - p_3 \frac{\partial g_3}{\partial x_3} - p_4 \frac{\partial g_4}{\partial x_3} \\ -p_2 - p_3 \frac{\partial g_3}{\partial x_4} - p_4 \frac{\partial g_4}{\partial x_4} \\ 0 \end{bmatrix}. \quad (27)$$

From (26), it is realized that the Hamiltonian is not a function of this additional state variable x_5 because the added state variable does not apparently exist in the state-space dynamics (19). Therefore, the last costate p_5 is constant [35].

Based on the principle of optimal control, the optimal joint torques were obtained by solving the following Equations [35]:

$$\frac{\partial H}{\partial \tau} = 0_{2\times1} \rightarrow \begin{cases} \tau_1 = -\frac{1}{R_1} \left(p_3 \frac{\partial g_3}{\partial \tau_1} + p_4 \frac{\partial g_4}{\partial \tau_1} \right) \\ \tau_2 = -\frac{1}{R_2} \left(p_3 \frac{\partial g_3}{\partial \tau_2} + p_4 \frac{\partial g_4}{\partial \tau_2} \right). \end{cases} \quad (28)$$

After the optimal torques of the shoulder and elbow joints were obtained at each moment, the optimal muscle forces should be determined using the second objective function and the Lagrangian method, which are explained in the next section.

3.2.2 | Optimal muscle forces

In this section, the optimal muscle forces are obtained at each moment using the instantaneous optimal joint torques in that moment. For this purpose, because of limitations in

the strengths of some muscles, the Lagrange method can be used for static optimization. In fact, the Lagrangian method is a suitable solution for finding the extrema of a mathematical function with some limitations. To minimize fatigue or the forces applied to the muscles, the following cubic cost function is considered:

$$J_2 = \frac{1}{2}\left(\sum_{i=1}^{6}\left(\frac{f_i(t)}{\text{PCSA}_i}\right)^3\right). \tag{29}$$

Because PCSA_i is the physiological cross-sectional area of the muscle i, $\alpha_i(t)\backslash\text{PCSA}_i$ represents the muscle stress of that muscle. It should be noted that muscle forces in the musculoskeletal system should always be positive. On the other hand, the muscle force for each muscle should not exceed the intolerance force value of that muscle. Therefore, the following constraint is considered for muscle forces in the Lagrange method:

$$0 \le f_i \le \sigma_{\max}\text{PCSA}_i \tag{30}$$

where $\sigma_{\max}$ is the maximum muscle stress value. As it was expressed, the muscle forces are related to joints torques by (3). Therefore, in order to obtain optimal muscle forces, the Lagrange function is defined as follows:

$$L = J_2 + \lambda(\tau - \mathbf{J}\mathbf{f}) \tag{31}$$

where the vector $\mathbf{f}(t) = [f_1(t), f_2(t), \ldots, f_6(t)]^T$ consists muscle forces and the vector $\lambda = [\lambda_1 \quad \lambda_2]$ has two elements that are called Lagrangian coefficients. The number of elements is the same as the number of Lagrangian constraint equations (Equation (3)).

By adding these two variables (λ_1, λ_2) with six variables related to the force of muscles (f_1, f_2, f_3, f_4, f_5, f_6) in the Lagrange function, there are eight variables in this optimization. Based on the Lagrange method, the optimal values of these variables are obtained by solving the 8 following equations:

$$\frac{\partial L}{\partial \lambda_j} = 0 \quad (j = 1, 2),$$
$$\frac{\partial L}{\partial \alpha_i} = 0 \quad (i = 1, \ldots, 6). \tag{32}$$

After solving the above equations, the optimal muscle forces are obtained. Thus, the optimal muscle activation can be recognized for any point-to-point movement. In fact, the function of the CNS can be investigated for these movements.

Now, this optimal trajectory of the proposed musculoskeletal arm model in the sagittal plane is assumed as a desired path of the fuzzy exponential sliding-mode controller presented in Section 3.1. Therefore, the patients' arms track the optimal point-to-point tasks in the sagittal plane.

4 | RESULTS

In this section, the simulation results are presented to evaluate the proposed method. The simulation results are expressed in three parts. First, the optimal human arm movement for arbitrary initial and final points is shown. Second, the arm's optimal trajectory is examined considering the experimental results. Finally, the nonlinear controller (FESMC) is implemented to move the arm in the manner similar to the desired optimal trajectory of the human arm, which is obtained from the optimal control criterion.

The forward and inverse kinematics of the considered two-link arm model in the sagittal plane were used in the simulation results. The position of the end effector in the Cartesian coordinate can be obtained by joint angles (θ_1, θ_2) as follows:

$$\begin{bmatrix} x \\ y \end{bmatrix} = \begin{bmatrix} L_1\sin(\theta_1) + L_2\sin(\theta_1 + \theta_2) \\ -L_1\cos(\theta_1) - L_2\cos(\theta_1 + \theta_2) \end{bmatrix}. \tag{33}$$

In addition, the inverse kinematics can be written as:

$$\begin{bmatrix} \theta_1 \\ \theta_2 \end{bmatrix} = \begin{bmatrix} \arctan2(x, -y) - \arccos\left(\frac{r^2 + L_1^2 - L_2^2}{2L_1 r}\right) \\ \arccos\left(\frac{L_1^2 - L_2^2 - r^2}{2L_1 L_2}\right) \end{bmatrix} \tag{34}$$

where $r = \sqrt{x^2 + y^2}$ and L_j ($j = 1$, 2) are the lengths of the upper arm and forearm segments, respectively.

4.1 | Simulation results of optimal criteria

To investigate the human-arm optimal point-to-point movements in the sagittal plane, the arbitrary initial and final states are considered as $x(0) = [20°, 30°, 0, 0]$ and $x(t_f) = [60°, 80°, 0, 0]$, respectively.

In addition, the boundary conditions and different arm and muscle parameters are mentioned in the previous sections. The final time is assumed to be 0.8 s, which is the average time of normal arm movements in the sagittal plane [36]. In the R matrix, the elements are considered to have equal value ($R_1 = R_2 = 100{,}000$).

Figure 4 shows the resulting optimal trajectory for the states ($x_1 = \theta_1$, $x_2 = \theta_2$, $x_3 = \dot{\theta}_1$, $x_4 = \dot{\theta}_2$). The lines and dashed lines represent the shoulder and elbow joints optimal trajectories and their derivatives (bell-shaped trajectory), respectively.

The two-dimensional (2D) optimal arm trajectory in Cartesian (x-y) coordinates between the initial and final points are demonstrated in Figure 5. As seen in the figure, this trajectory becomes a curved path by using the explained optimal criterion. In fact, the CNS also guides the segments to move along the curved paths in order to minimize the joint torques and muscle forces, and this is examined in the next section.
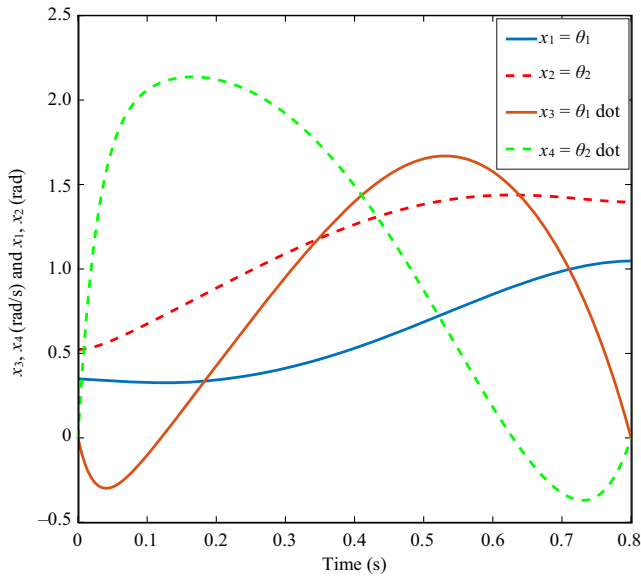
FIGURE 4 Optimal trajectories of arm point-to-point movement for joints and their derivatives in 0.8 seconds (states)
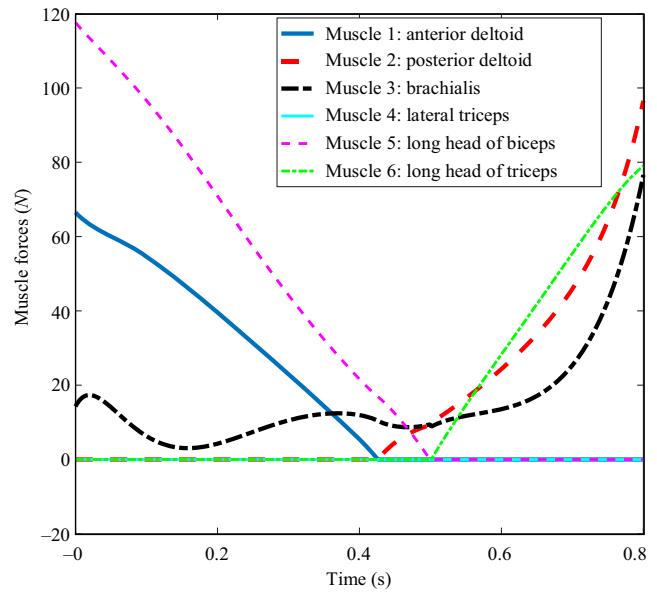

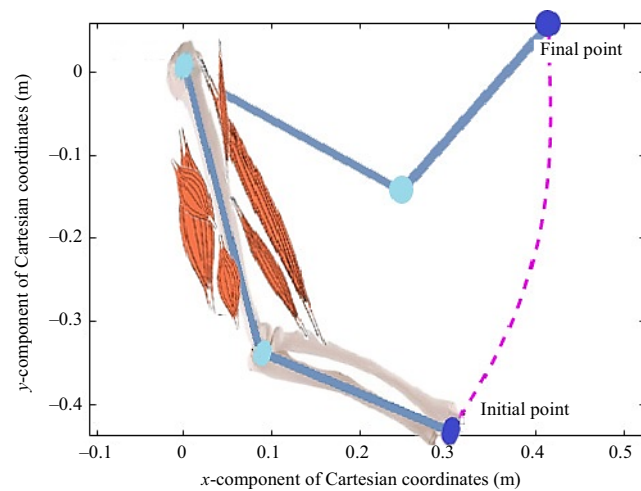**FIGURE 6** Optimal muscle forces for six muscles of proposed human musculoskeletal human arm model

FIGURE 5 Obtained optimal trajectory of arm movement in the sagittal plane between two specified points in Cartesian coordinates

FIGURE 7 Input torques to shoulder and elbow joints for the total duration

Figure 6 illustrates the optimal muscle forces for the six considered muscles that were obtained for this criterion. According to the figure, all of the muscle forces are positive (tensile). In addition, it can be seen that all muscles are activated in a substitution manner, which means that when one is activated, its pair is not activated and the magnitude of its force is zero. For example, in this arbitrary point-to-point movement when the anterior deltoid muscle (blue line) is activated, the posterior deltoid (red dash line) has a zero force. At about the middle of the trajectory, this activation is switched between these paired muscles. However, because of existing excessive muscle actuators, the lateral triceps muscle is not actuated in this movement, and its pair (brachialis muscle) is activated at all times for this movement.
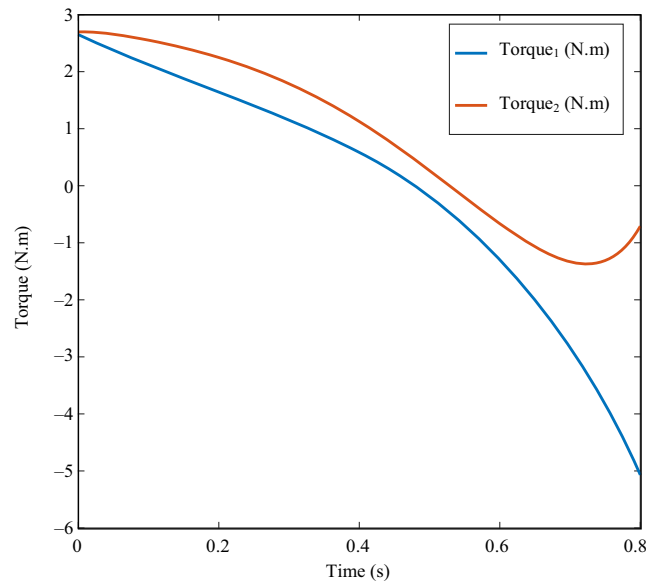
The input torques for shoulder and elbow joints are presented in Figure 7. By comparing Figure 6 and Figure 7, it is observed that the muscles that are activated in the initial phase of the movement (muscles 1 and 5) are agonistic muscles, which generate torques in the same direction of movement (positive torque). In addition, the muscles that are activated in the final phase of the movement (muscles 2 and 6) are antagonistic muscles, which generate torques in the direction opposite to the movement (negative torque).
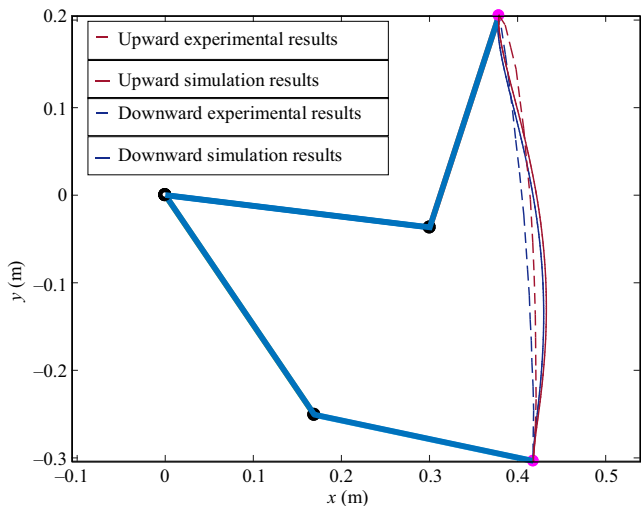
FIGURE 8 Comparison of simulation results and experimental results

4.2 | Evaluation of optimal trajectory results using experimental results

In this section, the experimental results for point-to-point human arm trajectory in the sagittal plane are obtained from Ref. [36]. Two points, namely 4 and 8, are considered as the initial and final points of the optimal simulation, respectively. A comparison of the results is shown in Figure 8 for upward and downward arm movements.

As seen in the figure, the upward trajectory (red line) is more curved than the downward trajectory. In fact, the downward motion is more convenient in the sagittal plane because of the gravitational effect. For upward movements, the arm should overcome the gravitational force. Therefore,
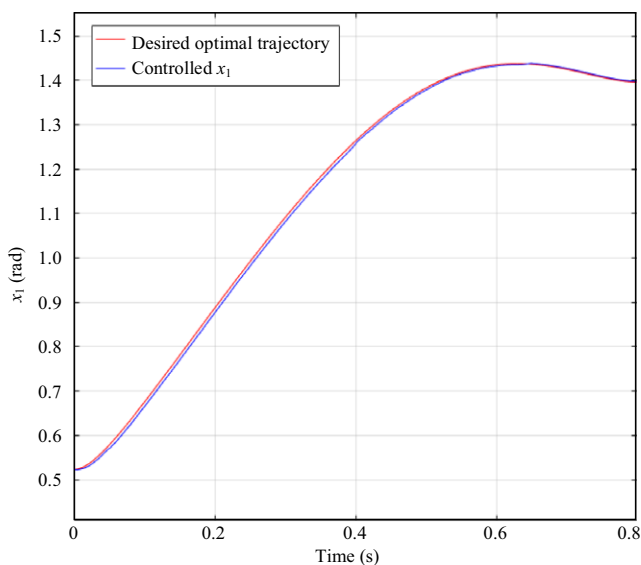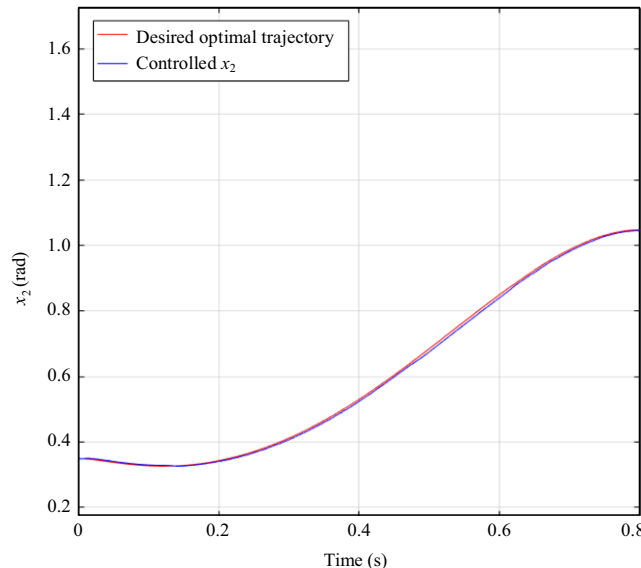

FIGURE 10 Response of fuzzy exponential sliding-mode control for the second state (elbow joint)

the joint torques become larger and the arm trajectory is more curved to satisfy the optimal criterion.

4.3 | Tracking results

The fuzzy exponential sliding-mode controller is applied for the proposed human arm model to track the optimal trajectory that was obtained in Section 4.1 of the results. The sliding-mode parameters were obtained from the exponential assumption criterion and fuzzy logic, which were explained previously. The tracking results for the shoulder and elbow joints are presented in Figure 9 and Figure 10, respectively. The suitable performance of this controller was investigated in our previous work [24].

5 | CONCLUSION

In this article, a 2-DOF musculoskeletal human arm model with six muscles was considered in the sagittal plane. In order to investigate the human arm trajectory, which is controlled by the CNS, two parallel optimal criteria were proposed for arm movements between two points. These two optimal criteria are the minimum muscle forces and the minimum joints torques. The optimal arm trajectory was obtained as the curve path, which is similar to experimental human arm results. The upward and downward arm trajectories are different from each other because in the sagittal plane, a gravitational force affects the arm movements. In addition, the optimal muscle forces were obtained, and it was seen that the biarticular, monoarticular, antagonistic, and agonistic muscles could be recognized from the results. The fuzzy exponential sliding-mode

FIGURE 9 Response of fuzzy exponential sliding-mode control for the first state (shoulder joint)

controller was designed to control the shoulder and elbow joints in order to achieve their optimal trajectories. Therefore, patients with spinal cord injuries can move their arms in a similar optimal manner as an intact human arm.

ORCID

Ramin Vatankhah 🆔 http://orcid.org/0000-0002-5529-5454

REFERENCES

1. W. Li, *Optimal control for biological movement systems*, Control **85** (2006), 156.

2. C. T. Freeman et al., *A model of the upper extremity using FES for stroke rehabilitation*, J. Biomech. Eng. **131** (2009), no. 3, 31011:1–31011:12.

3. B. I. Prilutsky, *Coordination of two- and one-joint muscles: Functional consequences and implications for motor control*, Motor Contr. **4** (2000), no. 1, 1–44.

4. M. Praagman et al., *The relationship between two different mechanical cost functions and muscle oxygen consumption*, J. Biomech. **39** (2006), no. 4, 758–765.

5. D. Tsirakos, V. Baltzopoulos, and R. Bartlett, *Inverse optimization: Functional and physiological considerations related to the force-sharing problem*, Crit. Rev. Biomed. Eng. **25** (1997), no. 4–5, 371–407.

6. N. Hogan, *An organizing principle for a class of voluntary movements*, J. Neurosci. **4** (1984), no. 11, 2745–2754.

7. T. Flash and N. Hogan, *The coordination of arm movements: An experimentally confirmed mathematical model*, J. Neurosci. **5** (1985), no. 7, 1688–1703.

8. Y. Uno, M. Kawato, and R. Suzuki, *Formation and control of optimal trajectory in human multijoint arm movement*, Biol. Cybernetics **61** (1989), no. 2, 89–101.

9. E. Nakano et al., *Quantitative examinations of internal representations for arm trajectory planning: Minimum commanded torque change model*, J. Neurophysiol. **81** (1999), no. 5, 2140–2155.

10. S. Ben-Itzhak and A. Karniel, *Minimum acceleration criterion with constraints implies bang-bang control as an underlying principle for optimal trajectories of arm reaching movements*, Neural Comput. **20** (2008), no. 3, 779–812.

11. R. M. Alexander, *A minimum energy cost hypothesis for human arm trajectories*, Biol. Cybern. **76** (1997), no. 2, 97–105.

12. Y. Ueyama and E. Miyashita, *Optimal feedback control for predicting dynamic stiffness during arm movement*, IEEE Trans. Ind. Electron. **61** (2014), no. 2, 1044–1052.

13. M. Sharif Shourijeh and J. McPhee, *Optimal control and forward dynamics of human periodic motions using Fourier series for muscle excitation patterns*, J. Comput. Nonlin. Dyn. **9** (2013), no. 2, 21005:1–21005:7.

14. W. Li and E. Todorov, *Iterative linearization methods for approximately optimal control and estimation of non-linear stochastic system*, Int. J. Contr. **80** (2007), no. 9, 1439–1453.

15. S. D. Farahani, *Prediction of closed-chain human arm dynamics in a crank-rotation task*, J. Biomechanics **49** (2016), no. 13, 2684–2693.

16. M. Zadravec and Z. Matjacic, *Planar arm movement trajectory formation: An optimization based simulation study*, Biocybern. Biomed. Eng. **33** (2013), no. 2, 106–117.

17. M. Sharifi, S. H. Pourtakdoust, and M. Parnianpour, *Optimal control of human-like musculoskeletal arm: Prediction of trajectory and muscle forces*, Opt. Contr. Applicat. Methods **38** (2017), no. 2, 167–183.

18. M. Sharifi, H. Salarieh, and S. Behzadipour, *Nonlinear optimal control of planar musculoskeletal arm model with minimum muscles stress criterion*, J. Comput. Nonlin. Dyn. **12** (2016), no. 1, 11014:1–11014:10.

19. K. Tahara and H. Kino, *Iterative learning control for a redundant musculoskeletal arm: Acquisition of adequate internal force*, IEEE/RSJ Int. Conf. Intell. Robots Syst., Taipei, Taiwan, October 18–22, 2010, pp. 234–240.

20. M. H. E. Balaghi et al., *Adaptive optimal multi-critic based neuro-fuzzy control of MIMO human musculoskeletal arm model*, Neurocomput. **173** (2016), no. 3, 1529–1537.

21. Y. W. Liao et al., *Multi-muscle FES control of the human arm for interaction tasks - Stabilizing with muscle co-contraction and postural adjustment: A simulation study*, IEEE Int. Conf. Intell. Robots Syst., Chicago, IL, USA, September 14–18, 2014, pp. 2134–2139.

22. J. H. Lilly and P. M. Quesada, *A two-input sliding-mode controller for a planar arm actuated by four pneumatic muscle groups*, IEEE Trans. Neural Syst. Rehabil. Eng. **12** (2004), no. 3, 349–359.

23. C. J. Fallaha et al., *Sliding-mode robot control with exponential reaching law, IEEE Trans*, Ind, Electron. **58** (2011), no. 2, 600–610.

24. Z. J. Shahbazzadeh, F. F. Ardakani, and R. Vatankhah, *Exponential sliding mode controller for a nonlinear musculoskeletal human arm model*, Int. Conf. Modeling, Simulation Appl. Opt., Sharjah, United Arab Emirates, April 4–6, 2017, pp. 1–5.

25. H. K. Khalil and J. Grizzle, *Nonlinear Systems*, Prentice Hall, Upper Saddle River, NJ, 2002.

26. H. Aschemann and D. Schindele, *Sliding mode control for a high-speed linear axis driven by pneumatic muscles*, Lect. Notes Contr. Inform. Sci. **407** (2010), 31–40.

27. K. Lochan, S. Suklabaidya, and B. K. Roy, *Sliding mode and adaptive sliding mode control approaches of two link flexible manipulator*, Proc. Conf. Adv. Robotics., Goa, India, July 2–4, 2015, pp. 58:1–58:6.

28. H. Q. Thinh Ngo, J.-H. Shin, and W.-H. Kim, *Fuzzy sliding mode control for a robot manipulator*, Artif. Life Robot. **13** (2008), no. 1, 124–128.

29. S. Moussaoui and A. Boulkroune, *Fuzzy approximation-based adaptive sliding-mode control scheme for underactuated systems*, Int. Conf. Contr., Eng. Inform. Technol., Tiemcen, Algeria, May 25–27, 2015, pp. 1–6.

30. K. R. S. Holzbaur et al., *Upper limb muscle volumes in adult subjects*, J. Biomech. **40** (2007), no. 4, 742–749.

31. W. M. Murray, T. S. Buchanan, and S. L. Delp, *The isometric functional capacity of muscles that cross the elbow*, J. Biomech. **33** (2000), no. 8, 943–952.

32. H. E. J. Veeger et al., *Parameters for modeling the upper extremity*, J. Biomech. **30** (1997), no. 6, 647–652.

33. P. Pigeon, L. Yahia, and A. G. Feldman, *Moment arms and lengths of human upper limb muscles as functions of joint angles*, J. Biomech. **29** (1996), no. 10, 1365–1370.

34. M. H. Rahman et al., *Control of an exoskeleton robot arm with sliding mode exponential reaching law*, Int. J. Contr. Autom. Syst. **11** (2013), no. 11, 92–104.

35. D. E. Kirk, *Optimal control theory: An introduction*, IEEE Trans. Autom. Contr. **17** (2004), 452.

36. C. G. Atkeson and J. M. Hollerbach, *Kinematic features of unrestrained vertical arm movements*, J. Neurosci. **5** (1985), no. 9, 2318–2330.

AUTHOR BIOGRAPHIES

Fateme Fotouhi Ardakani received her BS and MS degrees in mechanical engineering from the School of Mechanical Engineering, Shiraz University, Fars, Iran, in 2015 and 2018, respectively. Her MS degree was in the field of control and vibration. Her main research interests include biomechanics, nonlinear control, robotics, mechatronics, and optimizations.

Ramin Vatankhah received his BS degree in mechanical engineering from the Shiraz University, Shiraz, Iran, in 2007. He received his MS and PhD degrees in mechanical engineering from the Sharif University of Technology, Tehran, Iran, in 2009 and 2013, respectively. He is currently an assistant professor in the Department of Mechanical Engineering at Shiraz University. His research interests include nonlinear vibration, chaos control, evolutionary computation techniques, boundary control of partial differential equations, nonlinear control, and fuzzy system control.

Mojtaba Sharifi received his BSc degree in mechanical engineering from Shiraz University, Shiraz, Iran, in 2010, and his MSc degree in mechanical engineering from Sharif University of Technology, Tehran, Iran, in 2012. He also received the PhD degree from the School of Mechanical Engineering at Sharif University of Technology, and in 2016, he was part of a collaborative project in the Department of Electrical and Computer Engineering, University of Alberta, Canada, as a doctoral researcher. His research interests are the control of biomedical robotic systems, human-robot interaction (HRI), haptics, and biomechanical and biological systems.